



Inflow Turbulence and Leading Edge Roughness Effects on Laminar-Turbulent Transition on NACA 63-418 Airfoil

Paper

Özçakmak, Özge Sinem; Aagaard Madsen, Helge; Sørensen, Niels N.; Sørensen, Jens Nørkær; Fischer, Andreas; Bak, Christian

Published in:

Journal of Physics: Conference Series

Link to article, DOI:

[10.1088/1742-6596/1037/2/022005](https://doi.org/10.1088/1742-6596/1037/2/022005)

Publication date:

2018

Document Version

Publisher's PDF, also known as Version of record

[Link back to DTU Orbit](#)

Citation (APA):

Özçakmak, Ö. S., Madsen, H. A., Sørensen, N. N., Sørensen, J. N., Fischer, A., & Bak, C. (2018). Inflow Turbulence and Leading Edge Roughness Effects on Laminar-Turbulent Transition on NACA 63-418 Airfoil: Paper. *Journal of Physics: Conference Series*, 1037(2), [022005]. DOI: 10.1088/1742-6596/1037/2/022005

DTU Library

Technical Information Center of Denmark

General rights

Copyright and moral rights for the publications made accessible in the public portal are retained by the authors and/or other copyright owners and it is a condition of accessing publications that users recognise and abide by the legal requirements associated with these rights.

- Users may download and print one copy of any publication from the public portal for the purpose of private study or research.
- You may not further distribute the material or use it for any profit-making activity or commercial gain
- You may freely distribute the URL identifying the publication in the public portal

If you believe that this document breaches copyright please contact us providing details, and we will remove access to the work immediately and investigate your claim.

PAPER • OPEN ACCESS

Inflow Turbulence and Leading Edge Roughness Effects on Laminar-Turbulent Transition on NACA 63-418 Airfoil

To cite this article: Ö S Özçakmak *et al* 2018 *J. Phys.: Conf. Ser.* **1037** 022005

View the [article online](#) for updates and enhancements.

Related content

- [Investigation of the effect of inflow turbulence on vertical axis wind turbine wakes](#)
P Chatelain, M Duponcheel, S Zeoli et al.
- [Results of the research project AssiSt](#)
Timo Kühn, Andree Altmikus, Hussam Daboul et al.
- [An asymptotic analysis of the laminar-turbulent transition of yield stress fluids in pipes](#)
Tim G. Myers, Sarah L. Mitchell and Paul Slatter



IOP | ebooks™

Bringing you innovative digital publishing with leading voices to create your essential collection of books in STEM research.

Start exploring the collection - download the first chapter of every title for free.

Inflow Turbulence and Leading Edge Roughness Effects on Laminar-Turbulent Transition on NACA 63-418 Airfoil

Ö S Özçakmak, H A Madsen, N N Sørensen, J N Sørensen, A
Fischer, C Bak

Technical University of Denmark, DTU Risø Campus, Frederiksborgvej 399, DK 4000
Roskilde, Denmark

E-mail: ozsi@dtu.dk

Abstract.

The surface imperfections and the inflow turbulence in real operational conditions can cause significant deviations from the predicted wind turbine aerodynamic performance and energy yield. In this study, particular emphasis was placed on the effect of these parameters on the laminar-turbulent transition on wind turbine blades. For this purpose, the DAN-AERO wind tunnel measurements, with high frequency microphones flush mounted on the both suction and pressure sides of the NACA 63-418 airfoil profile, were used. Typical operating condition Reynolds numbers, turbulence grid and boundary layer control devices on the surface were implemented. The results indicate a high dependency of the transition process on these parameters. The analyses show that the critical height of the leading edge roughness (LER) is to be met in order to have a bypass transition to turbulent flow at the angle of attacks, where the stagnation point is upstream of the LER location. The transition location moves closer to the leading edge with increasing Reynolds number when the roughness height is smaller than the critical height. Inflow turbulence is observed to have a larger effect on the transition location than the predicted numerical results.

1. Introduction

The prediction and the understanding of the laminar to turbulent transition behaviour has a significant role in the design process of wind turbines. The transition location on wind turbine is influenced by several parameters including the roughness and inflow turbulence.

Roughness on the wind turbine blades can occur due to manufacturing process or long service periods (ageing). Moreover, natural accumulations such as dirt and contamination due to insects, ageing, sand, ice, smog, rain or erosion occur during operation. This contamination changes the aerodynamic shape of the wind turbine blades and can lead to a lower performance and power production. The accumulation or erosion along the leading edge can cause power output drop to 40 % of its clean value [1] and 25 % loss in annual energy production [2]. The decrease in performance and unpredictable stall behaviour due to dust accumulation on the blade is one of the most critical problem for wind turbines [3].

When the roughness height, so the roughness Reynolds number reaches a critical value, transition moves forward from its natural location close to the roughness [4]. If the roughness



height is equal to the critical size, the turbulent spots start to form at the roughness location and form into turbulent flow downstream of the roughness. If the roughness height is higher than the critical height, then fully turbulent flow occurs at the roughness location [5]. The impact of roughness on airfoil performance depends on the roughness size with respect to the boundary layer thickness, the type of the roughness, the airfoil shape and the Reynolds number [3]. The airfoil thickness causes higher pressure gradients at the aft region on the airfoil upper surface. The thickness in combination with the leading edge contamination can cause earlier transition of the laminar boundary layer and early turbulent separation, and thus a significant decrease in maximum lift coefficient [6].

Furthermore, the interest in the effect of free stream turbulence on the onset of the laminar to turbulent transition has increased lately [7]. In addition to the surface roughness, the inflow turbulence experienced by the wind turbine blades in the free atmosphere can cause severe decreases in performance of the wind turbine.

There have been studies on LER on wind turbine blades and wind turbine airfoils which are mostly concentrated on low Reynolds numbers [8] or analyzed by force or hot-film measurements [9]. As the wind turbines grow in size, there is a need for characterization of the transition behaviour of the wind turbine blades at high Reynolds numbers. Moreover, transition location can be precisely captured by the use of high frequency response instruments in experiments.

In this study, experimental data obtained from DAN-AERO [10] [11] wind tunnel experiments are analysed. Surface pressure fluctuations were measured by high frequency microphones placed chordwise on both the suction and pressure sides of the airfoil surface. The airfoil used in the experiments was manufactured identical to the cross-section at 37 meters radius from the hub of LM38.8 blade of the NM80 turbine. Both time and frequency domain analyses are performed for surface pressure readings from microphones in order to detect the transition location on the airfoil. The transition position is calculated by the maximum derivative of the sound pressure levels (SPL) along the chordwise direction and by the first moment of the spectra.

The effect of the inflow turbulence is analysed by means of a high solidity turbulence grid, which raises the turbulence intensity level from 0.1 % to about 1.2 % in the wind tunnel. The angle of attack (AOA) and Reynolds number are varied and boundary layer control devices (zigzag tape and trip wire) are applied for simulating LER. The effects of LER and inflow turbulence on the laminar to turbulent transition are examined.

2. Experimental Method and Data Analysis

In the experiments, the NACA 63-418 airfoil profile, with flush mounted microphones both on the suction and the pressure sides, is used. The airfoil belongs to the most outward section (37 meters from the hub) of the LM 38.8 blade of NM80 wind turbine. The chord of the model is 0.9 meters and it is manufactured identical to the section of the LM 38.8 blade. For the analysis, 41 high frequency microphones on the suction side and 25 on the pressure side are used. The microphones have a diameter around 4 mm and were installed about 1 mm below the surface of the airfoil. These high frequency microphones are distributed also in the span-wise direction to reduce the disturbance from the upstream microphones. The airfoil profile and microphone positions are illustrated in Figure 1.

The experiments were carried out at the LM Glassfiber Low Speed Wind Tunnel which has a test section width of 1.35 m, a height of 2.70 m and a length of 7 meters [12]. The turbulence intensity of the LM wind tunnel is around 0.1 % which plays an important role for inflow conditions and amplification factor (N) chosen for the numerical calculations.

Experiments are conducted at Reynolds numbers of typical operating conditions of a horizontal axis wind turbine ($1.6 \cdot 10^6$, $3 \cdot 10^6$, $4 \cdot 10^6$, $5 \cdot 10^6$ and $6 \cdot 10^6$). The angle of attack is varied from -15 to 16 degrees with one degree and half a degree increments. The data are sampled at 50000 Hz for 10 seconds. The test cases are tabulated in Table 1.

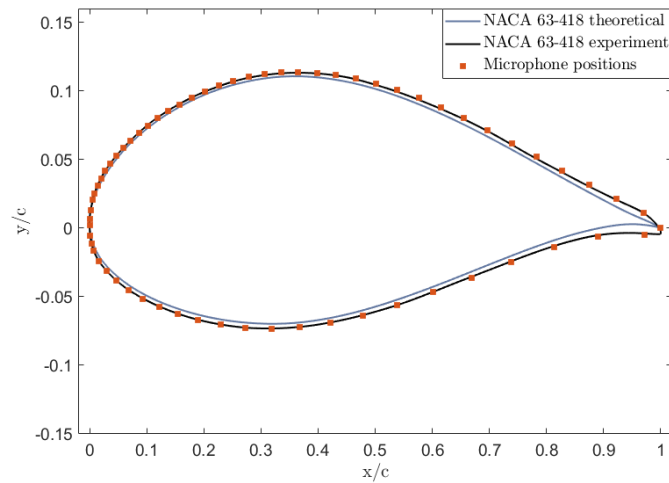


Figure 1. NACA 63-418 theoretical, experimental airfoil geometry and microphone positions.

Table 1. Test Cases

Parameter	Description
Reynolds numbers	$1.6 \cdot 10^6$, $3 \cdot 10^6$, $4 \cdot 10^6$, $5 \cdot 10^6$, $6 \cdot 10^6$
Angle of attack	-15 to 16 degrees
Zigzag tape	0.4 mm at 1% chord suction side
Bump tape	0.1 mm at 2% chord suction side
Turbulence grid	100 x 100 mm mesh size

The surface roughness close to the leading edge on the upper surface is enforced by the bump tape and 90° zigzag tape boundary layer control mechanisms. The normalized roughness height with respect to 0.9 m chord for bump tape is $1.1 \cdot 10^{-4}$ and for the zigzag tape $4.4 \cdot 10^{-4}$.

The inflow turbulence is created by a turbulence grid which has a 100 mm x 100 mm mesh size with a 40 mm width and 3 mm thickness. Hot wire analysis showed that when the turbulence grid is installed, the turbulence intensity is around 1-1.2 % [13]. This corresponds to a N factor of 2.62-2.19. The following equation is used to determine N values [14];

$$N = -8.43 - 2.4 \cdot \ln(T.I.\%/100). \quad (1)$$

The N factor is chosen as 8 for the low turbulence intensity case (measurements without the turbulence grid), which corresponds to turbulence intensity value of 0.106%. Moreover, N factors of 0.2, 0.3, 1, 2 and 3 are used for the high turbulence intensity case (measurements with the turbulence grid) for numerical calculations. The model in the LM Wind Tunnel with bump tape (left), turbulence grid (right-top) and surface mounted microphones (right-bottom) are presented in Figure 2.

The transition location from experiments is calculated by two methods; sudden chordwise increase in sound pressure level and first moment of the power spectral density (PSD). The standard deviation (σ or P_{rms}), which can be considered as the total energy of the pressure fluctuations, has been calculated from the pressure spectra;

$$P_{rms}^2 = \int_{f1}^{f2} PSD df, \quad \sigma = \sqrt{P_{rms}^2}. \quad (2)$$



Figure 2. NACA 63-418 Airfoil in LM Wind Tunnel with bump tape(left), Turbulence grid(right-top) and Surface Microphones(right-bottom).

The f_1 and f_2 are the lower and upper frequency boundaries of the interested spectra region. When transition from laminar to turbulent flow occurs, there is a chordwise increase in the σ value. It should be noted that the PSD generated here is already doubled in magnitude and one sided. The first method used in the transition detection is based on the maximum derivative of the sound pressure levels (L_p) calculated with a reference pressure value of $P_{ref} = 20 \mu \text{ Pa}$;

$$L_p = 20 \cdot \log_{10}\left(\frac{P_{rms}}{P_{ref}}\right). \quad (3)$$

The second transition detection method is based on the first moment of the spectra, which is calculated by Equation 4. In this method, the high frequency content of the spectra, where the transition peaks are expected, is amplified by multiplication by the frequency (f). Later, it is seen that if the inflow turbulence levels are high, this method may provide misleading results. Therefore, in the current analysis, both SPL derivative and first moment of the spectra methods are applied and validated by the PSD plots.

$$f_\mu = \frac{\int_{f_1}^{f_2} f \cdot PSD df}{\int_{f_1}^{f_2} PSD df} \quad (4)$$

The frequency range is selected as $f_1 = 2000 \text{ Hz}$ to $f_2 = 7000 \text{ Hz}$ since at the frequencies higher than 7000 Hz , pinhole placement of the microphones causes resonance in the tubing system that results in a bump in the spectra. Furthermore, frequencies lower than 2000 Hz are not included; large eddies in stall and inflow turbulence are present below that frequency, which causes an increase in the low frequency content.

The positions of the microphones on the airfoil surface are identical to the ones placed on the section of the LM 38.8 blade. Due to this microphone placement, it is believed that some upstream microphones create a turbulent wedge that affects the downstream microphones. This was taken into consideration during the analysis by examining the spectra and microphone placement. The biggest increase in the sound pressure levels or first moment of the spectra determines the transition location calculated from the experiments. Depending on the distance between the microphones and flow conditions, this location can belong either to transition in process or to the point where turbulent flow is first achieved.

3. Results and Discussion

3.1. Inflow Turbulence

The pressure PSD at several chordwise positions at the suction side at $Re=3 \cdot 10^6$ and $AOA=0^\circ$ without (a) and with (b) turbulence grid are presented in Figure 3. When the turbulence grid is installed, microphones close to the leading edge contain high energy at low frequency frequencies due to the inflow turbulence. Thus, the energy difference between laminar and turbulence spectra decreases significantly, which makes it harder to detect the transition location. This difference decreases further as the Reynolds number increases from $Re=1.6 \cdot 10^6$ to $Re=3 \cdot 10^6$ and above. On the other hand, when the turbulence intensity is low in the wind tunnel, there is a significant energy difference between laminar and turbulent spectra. Moreover, the peaks due the wind tunnel noise are stronger when the turbulence grid is installed.

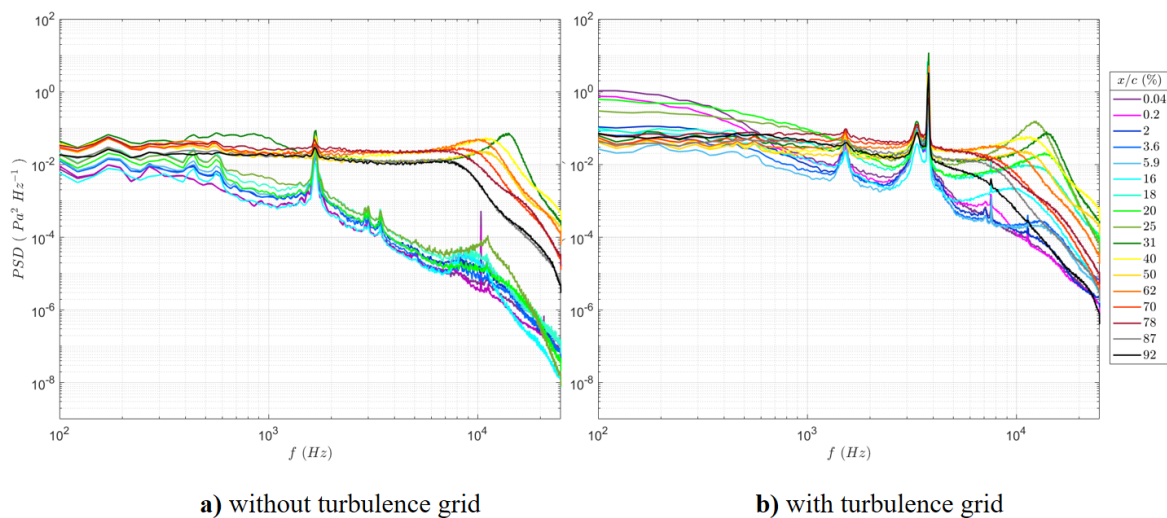


Figure 3. PSD at several chordwise positions on the suction side of the clean airfoil with (a) and without (b) a turbulence grid at $Re=3 \cdot 10^6$ at $AOA=0^\circ$.

The transition locations determined from experiments with and without turbulence grid cases for the clean airfoil at a $Re=3 \cdot 10^6$ are presented for various angle of attack values in Figure 4. XFOIL analyses are performed for various N factors that are determined from the turbulence intensity of the wind tunnel with and without the grid. It can be seen that, for the case without the grid, the XFOIL results fit with the experiments, except for the middle angle of attack range. It is observed from the experimental data that the transition point suddenly moves to 27% chord on the suction side, at -5 degree angle of attack. This is believed to be due to the microphone placement (the microphones in the wake of upstream ones) in combination with the adverse pressure gradients and cavity around certain microphones. These combined conditions cause premature boundary layer transition. For the configuration with the turbulence grid, it is seen that as the inflow turbulence increases, the transition location moves much further forward close to the leading edge than predicted by the numerical results. The high turbulence intensity case fits with the experiments for $N=0.3$ for angle of attack values higher than 3 degrees. This N value (0.3) is much lower than the expected N value at 2.4 for the measured turbulence intensity of the wind tunnel with fine turbulence grid.

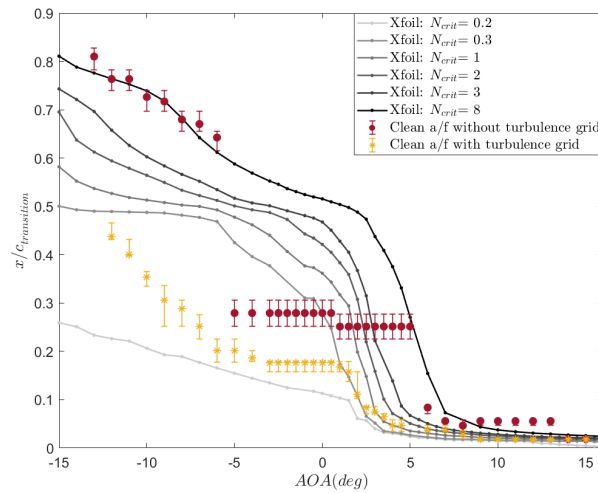


Figure 4. Transition locations for various angle of attack values with and without a turbulence grid for clean airfoil upper surface at $Re=3 \cdot 10^6$.

3.2. Leading Edge Roughness

Transition locations for the clean airfoil, airfoil with the zigzag tape and with the bump tape on the suction side are presented in comparison with the XFOIL results in Figure 5. Transition from a laminar to a turbulent boundary layer is forced at the zigzag and bump tape locations to simulate the effect of surface roughness in XFOIL calculations. There have been low speed wind tunnel test studies, which show that the placement of zigzag and straight tapes causes earlier turbulence transition [15]. It is seen from the zigzag tape experimental results that the transition behaviour is the similar to that of the clean case until the stagnation point moves upstream from the LER (zigzag tape) location as the angle of attack increases. When the leading edge roughness is downstream of the stagnation point then the bypass transition occurs and flow becomes turbulent. However, it is seen that the critical height to trigger bypass transition is not met with 0.1 mm bump tape; it indeed shows a similar trend with the clean profile for the angle of attack values less than 2 degrees. Moreover, it is seen that for the zigzag tape case, XFOIL results fit with the experiments.

The calculated transition locations for the bump tape, which is applied at 2 % chord at the suction side, for 5 different Reynolds numbers, are presented in Figure 6 (left). The current data show that the effect of the bump tape highly depends on the Reynolds number. As the Reynolds number increases, the transition location moves further upstream closer to the leading edge for all AOA cases.

It is known that zigzag tape is a very effective roughness element that does not only change transition location but can also increase the momentum thickness of the turbulent boundary layer and can change airfoil characteristics [6]. The Reynolds number dependency for the zigzag tape is presented in Figure 6 (Right). At low angles of attack from -15 to -6 degrees, increasing Reynolds number causes earlier transition. The zigzag tape triggers transition sharply after -6 degrees. As the certain angle of attack value is reached for bypass transition, the transition behaviour becomes independent of the Reynolds number with a zigzag tape.

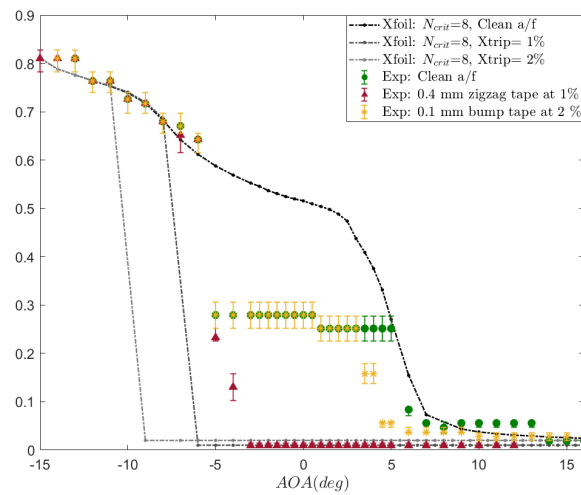


Figure 5. Transition locations for various angle of attack values at $Re=3 \cdot 10^6$: for clean airfoil, for the airfoil with the zigzag tape and with the bump tape.

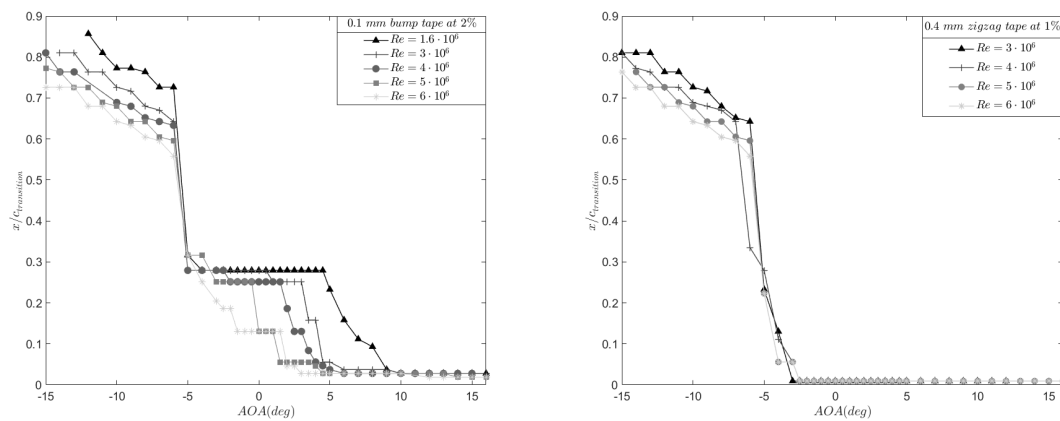


Figure 6. Transition locations for various angle of attack values at different Reynolds numbers: *Left* : with a 0.1 mm bump tape at 2 % chord, *Right*: with a 0.4 mm zigzag tape at 1 % chord on the suction side of the profile.

4. Conclusion

The transition characteristics of NACA 63-418 airfoil profile manufactured based on the specific section of the LM 38.8 blade of the NM80 wind turbine from the DAN-AERO experiments, are analysed under varying inflow turbulence and leading edge roughness conditions. It is seen that the roughness effects become more severe with increasing free stream velocity. Therefore, if the free stream velocity is increased, then the height of the roughness element can be reduced to trigger bypass transition. It was observed in the previous studies for different airfoils that 0.1 mm bump tape on 2 % chord does not have an influence on maximum lift or lift to drag ratio [16]. It is seen also in the current analysis that bump tape does not affect the laminar to turbulent boundary layer transition since the normalized roughness height of $1.1 \cdot 10^{-4}$ is below the critical

roughness height for this airfoil in the range of 1.6 to 6 million Reynolds number. Zigzag tape, in contrast, triggers transition for the angle of attack cases where stagnation point is upstream of the roughness element. Therefore, as the critical height of the leading edge roughness is exceeded, the transition from laminar to turbulent flow occurs by the bypass mechanism at the condition that the stagnation point stays forward of the LER location. In this condition, the transition location becomes independent of the Reynolds number.

Increased inflow turbulence forces the transition points closer to the leading edge and, expectedly, skin friction drag increases due to the larger portion of the airfoil surface covered by a turbulent flow. The similar behaviour is observed with increasing angle of attack on the suction side. The detection of the transition locations under high inflow turbulence is difficult due to the high wind tunnel noise especially for the microphones close to the leading edge. When the transition location is close to the leading edge, leading edge noise can interact with the transition related noise. Moreover, inflow turbulence combined with an increasing Reynolds number induces instabilities in the flow. This causes turbulent spots on some microphones, which affects the downstream ones depending on the spanwise location of the microphones. Thus, for high inflow turbulence measurements, high frequency microphone analysis should be performed by placing less microphones in order to reduce interaction. Moreover, microphones should be placed spanwise with a wider angle than the turbulence wedge angle caused by the existence of the microphone itself. To sum up, it is seen that the Reynolds number, inflow turbulence and surface roughness have a significant effect on the transition location, therefore on the aerodynamic performance of the wind turbine blades.

References

- [1] Hansen A C and Butterfield C P 1993, Aerodynamics of Horizontal-Axis Wind Turbines. *Annu. Rev. Fluid Mech.* **25** : 115-149.
- [2] Sareen A, Sapre C A and Selig M S 2014, Effects of leading edge erosion on wind turbine blade performance. *Wind Energy* **17** : 1531-1542.
- [3] Khalfallah M G and Koliub A M 2007, Effect of dust on the performance of wind turbines. *Desalination* **209** : 209-220.
- [4] Braslow A L, Hicks R M and Harris, Jr. R V 1966, Use of Grit-Type Boundary-Layer-Transition Trips on Wind-Tunnel Models *NASA Technical Report*
- [5] Braslow A L and Knox E C 1958, Simplified Method for Determination of Critical Height of Disturbed Roughness Particles for Boundary-Layer Transition at Mach Numbers from 0 to 5 *NACA* **4363**
- [6] van Rooij R P J O M and Timmer W A 2003, Roughness Sensitivity Considerations for Thick Rotor Blade Airfoils. *ASME* **125**.
- [7] Biau D, Arnal D and Vermeersch O 2007, A transition prediction model for boundary layers subjected to free-stream turbulence. *Aerospace Science and Technology* **11** : 370-375.
- [8] Giguère P and Selig M S 1998, Aerodynamic Effects of Leading Edge Tape on Aerofoils at Low Reynolds Numbers *Wind Energy* **2** : 125-136.
- [9] Marzabadi F R and Soltani M R 2013, Effect of leading-edge roughness on boundary layer transition of an oscillating airfoil *Scientica Iranica Transactions B: Mechanical Engineering* **20** : 508-515.
- [10] Troldborg N, Bak C, Madsen H Aa and Skrzypinski W R (2013). DANAERO MW II: Final Report. *DTU Wind Energy*.
- [11] Madsen H Aa, Bak C, Paulsen U S, Gaunaa M, Fuglsang P, Romblad J, Olesen NA, Enevoldsen P, Laursen J and Jensen L, 2010. The DANAERO MW Experiments. *Danmarks Tekniske Universitet, Risø Nationallaboratoriet for Bredlygtig Energi*.
- [12] Fuglsang, P 2006, LM Wind Tunnel
- [13] Fisher A 2012, Hot Wire Anemometer Turbulence Measurements in the wind Tunnel of LM Wind Power. *Wind Energy Department, Technical University of Denmark* **E-0006**
- [14] Mack L M 1977, Transition and Laminar Stability *NASA Jet Propulsion Laboratory*
- [15] Soltani M R, Birjandi A H and Seddighi Moorani M 2010, Effect of surface contamination on the performance of a section of a wind turbine blade. *Scientica Iranica Transactions B: Mechanical Engineering* **18** : 349-357.
- [16] Bak C, Gaunaa M, Olsen A S and Kruse E K 2016, What is the critical height of leading edge roughness for aerodynamics? *Journal of Physics: Conference Series* **753**